Superheat Control of an Inverter-driven Heat Pump Using PI Control Algorithm

Jongmin Choi* and Yongchan Kim**

Key words: Inverter-driven heat pump, EEV, Superheat, PI control, Feedback control, Feedforward control

Abstract

The performance of an inverter-driven water-to-water heat pump with an electronic expansion valve (EEV) was measured as a function of compressor frequency, load conditions, and EEV opening. Based on the test results, a controller using proportional integral (PI) feedback or PI feedforward algorithm was designed and tested to investigate capacity modulation and transient response control of the system. Although the relation between superheat and EEV opening of the heat pump showed nonlinear characteristics, a control gain obtained at the rated frequency was applicable to various operating conditions without causing large deviations. When the simple PI feedback control algorithm was applied, a large overshoot of superheat and wet compression were observed due to time delay effects of compressor frequency. However, applying PI feedforward control scheme yielded better system performance and higher reliability, compared to the PI feedback algorithm.

Nomenclature

EO : EEV opening [step]
F : compressor frequency [Hz]
G : transfer function
K_e : steady state gain [℃/step]
K_I : integral gain [step/℃ · s]
K_p : proportional gain [step/℃]
$\dot{Q}_{req}$: cooling capacity [kW]
SH : superheat [℃]
SC : subcooling [℃]
T_{ci} : secondary fluid temperature at the inlet of the condenser [℃]
T_{ei} : secondary fluid temperature at the inlet of the evaporator [℃]
T_{eo} : secondary fluid temperature at the outlet of the evaporator [℃]
T_s : sampling time [s]

Greek symbols

τ : time constant [s]
τ_d : delay time [s]

* Thermal Machinery Group, NIST, MD, USA
** Department of Mechanical Engineering, Korea University, Seoul, Korea

1. Introduction

An inverter-driven heat pump modulates the capacity using compressor frequency control with respect to a building load.[1] The inverter-driven heat pump covers wider capacity range than a constant speed heat pump. In addition, it provides not only precise capacity control but also energy conservation and possibility of application to an intelligent building system.[2]

The performance of expansion devices plays a crucial role on the inverter-driven heat pump since the refrigerant flow rate control by employing an appropriate expansion device becomes significant in the inverter-driven system. Therefore an electronic expansion valve (EEV), which has superior performance to a capillary tube, has been implemented in an inverter-driven heat pump.[3-5]

Hewitt et al.[6] compared the performance of a TXV with an EEV in a refrigeration system. He reported that a solenoid expansion valve produced the best mass flow control. Matsuoka and Nagatomo[7] derived a step response from the transient superheat characteristics as a function of compressor frequency, indoor fan speed, and EEV opening. Nancy[8] investigated the system performance with a variation of load and evaporator exit superheat.

In this study, the performance of an inverter-driven heat pump with an EEV was measured with respect to load conditions. Based on the performance tests, the characteristics of capacity modulation and optimal control were investigated. In order to adjust compressor speed and EEV opening, control parameters and control algorithm were selected and derived, respectively. A controller applying PI feedback or PI feedforward algorithm was constructed based on the test results, and then its performance was tested with a variation of load conditions.

2. Test setup and procedure

A schematic diagram of the experimental setup for the inverter-driven heat pump is shown in Fig. 1. The heat pump consists of a horizontal variable speed scroll compressor, two double tube type heat exchangers (evaporator and condenser) and an electronic expansion valve driven by a stepping motor. The condenser and evaporator had a counter flow pat-

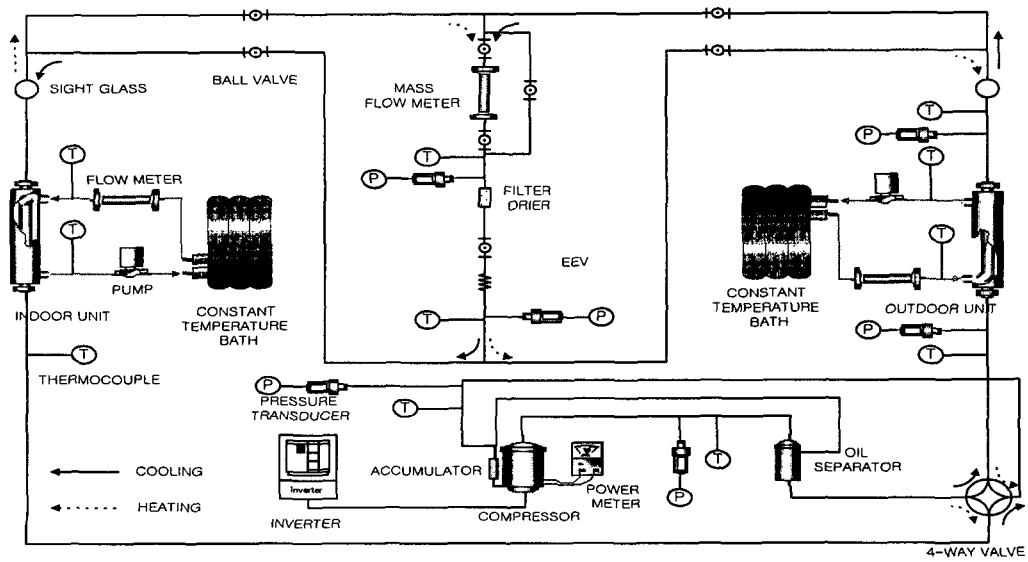

Fig. 1 Schematic diagram of an experimental water-to-water heat pump system.

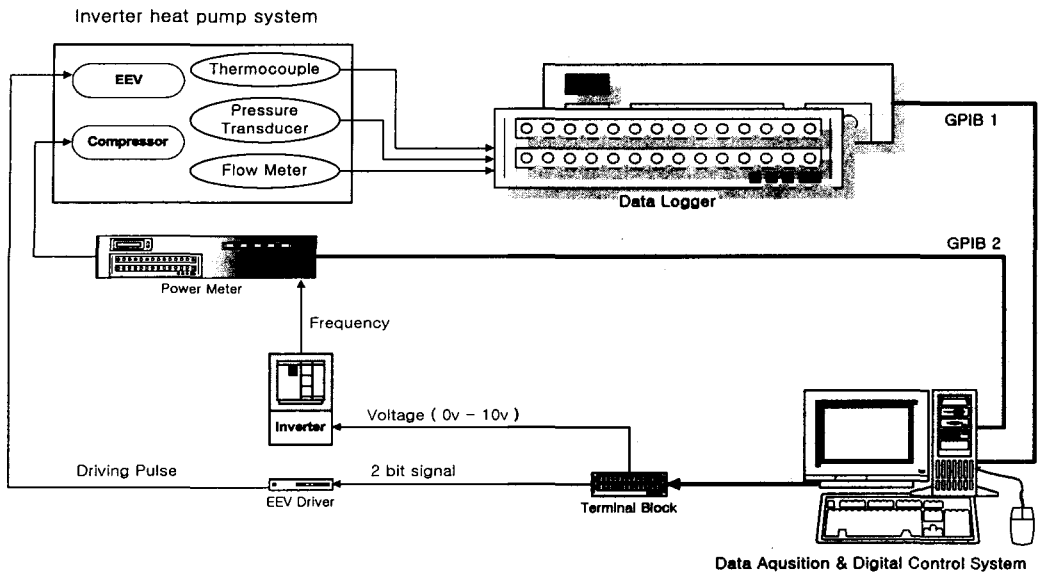

Fig. 2 *Schematic diagram of measurement and control system.*

tern between secondary fluid and refrigerant. Ethylene-glycol was selected as a heat source and sink for the heat pump because of its simplicity of capacity measurement. The secondary flow loops for the evaporator and condenser includes a magnetic pump and a constant temperature bath. Each constant temperature bath contains a refrigeration system and an electric heater. The pump and manual needle valve controls the flow rate supplied to the condenser and evaporator to establish test conditions.

A schematic diagram of the measurement and control unit is shown in Fig. 2. The flow rates of the refrigerant and secondary fluid, temperatures and pressures of the secondary fluid and the major points in the system, and power consumption are measured in the test rig. Compressor speed was controlled by a controller including a computer and a D/A board, and the EEV opening was adjusted by an EEV driver.

The performance of the heat pump was measured with a variation of second fluid temperatures at the inlets of the condenser and evaporator, compressor speed, and EEV opening in the cooling mode. Table 1 summarizes test conditions.

Test data was monitored by using a real time data acquisition system. Superheat, subcooling, cooling capacity, and COP were calculated using REFPROP,[9] and then those values were applied to the control system as input data. Once the variations of temperature and pressure at the inlet and outlet of the compressor, and the refrigerant flow rate were within ±0.25℃, ±5 kPa, ±0.5 kg/h, respectively, during 5 minutes, the data were stored for every two seconds in 5 minutes. The uncertainty of cooling capacity was approximately ±3.1%.

Table 1 Test conditions

Condenser	Inlet temperature	30℃, 34℃, 38℃
	Flow rate	7 lpm
Evaporator	Inlet temperature	22℃, 25℃, 28℃
	Flow rate	9 lpm
Compressor frequency		30 Hz, 45 Hz, 60 Hz, 90 Hz
EEV		Controlled for the maximum COP

3. Control system

The setpoint of superheat was determined based on the steady state performance tests for the inverter-driven heat pump. In addition, a control algorithm was developed from the transient response characteristics of the superheat according to EEV opening. Both the capacity and refrigerant flow rate were simultaneously controlled with a variation of disturbance and load by adjusting compressor speed and EEV opening.

The secondary fluid temperatures at the inlets of the evaporator and condenser were selected as a disturbance in the estimation of controller performance. The control program calculates the required cooling capacity as a function of secondary fluid temperature and compressor speed. At a given compressor speed, the EEV opening was controlled to obtain a maximum steady state performance and a stable transient system response using PI feedback or PI feedforward control algorithm. In case of PID (Proportional Integral Differentiation) control, there may exist an unstability of the system control and the complexity due to noise filtering when the feedback system has a measurement noise. Furthermore, since the transient response of superheat according to an EEV opening is the 1st order system, the PI control scheme is appropriate for the 1st order system.[10 12] The EEV opening and the variation of superheat were modelled by the 1st order system as given in Eq. (1). The control gain was determined by the Ziegler-Nichols[2,13] method which is very efficient method in a heat pump system.[2] The method includes three steps as follows: (1) the superheat was measured with a variation of EEV opening, (2) the time constant and time delay were determined by a graphical method, and (3) the control gain was evaluated from time constant and time delay, and retuning process.[2,10]

$$\frac{SH(s)}{EO(s)} = \frac{K_e}{1+\tau s} e^{-\tau_d s} \tag{1}$$

where, $K_e = \frac{\triangle SH}{\triangle EO}$.

The control algorithm is composed of two parts: (1) compressor speed is selected to match a required cooling capacity, and (2) a stabilization of transient response and an optimization of the system were obtained by adjusting refrigerant flow rate using an EEV control.

In the PI feedback control, the compressor speed was adjusted using a correlation of compressor frequency as a function of secondary fluid temperatures entering into the condenser and evaporator. In addition, the EEV opening was controlled by comparing the feed-

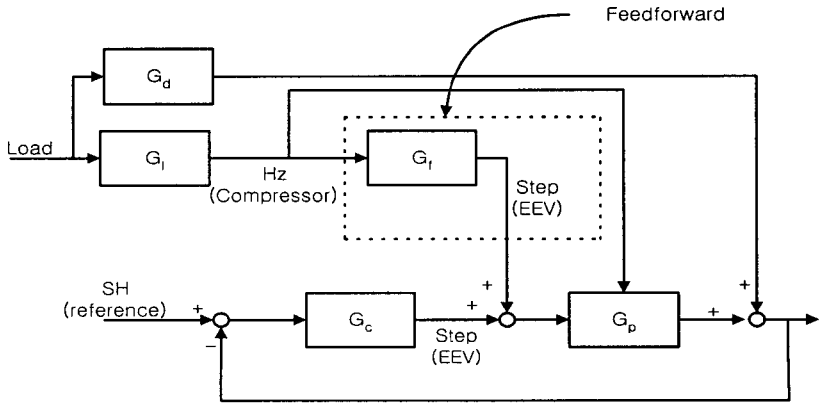

Fig. 3 Block diagram of the controller.

back superheat with the setpoint of superheat. In the PI feedforward control, the control algorithm of EEV opening was inserted into the PI feedback algorithm to compensate the effects of compressor frequency on the superheat in advance. Fig. 3 shows a block diagram of the control system.

The controller (G_c) for adjusting superheat uses the PI control scheme, and the output will be EEV opening. The variation of the load disturbs superheat through the G_d, and the change of compressor speed alters plant (G_p) through the G_I in the PI feedback controller. However, in the PI feedforward control, the EEV opening is adjusted through G_f prior to the feedback control of superheat to take account for the variation of compressor speed.

4. Results and discussion

4.1 Performance of the system

Figs. 4 and 5 show the variations of cooling capacity, subcooling and superheat as a function of secondary fluid temperature in the condenser when the EEV opening is adjusted to maximize the COP of the system. Cooling capacity increases with an increase of compressor speed at constant loads in the condenser and evaporator. However, the cooling capacity decreases with an increase in the condenser load because the temperature difference between the refrigerant and the secondary fluid drops in the evaporator. Besides, this causes the existence of two-phase refrigerant at the evaporator exit. Therefore, the EEV opening needs to be closed to reduce the refrigerant flow rate and to maintain appropriate superheat at the exit of the evaporator. Generally, as the EEV opening decreases subcooling drops but the superheat remains nearly constant because a drop of temperature difference between refrigerant and secondary fluid in the condenser is larger than that in the evaporator. Therefore, it is more reasonable to use superheat as a control parameter with a variation of condenser load as compared to the use of subcooling.

Fig. 6 shows the variations of superheat and subcooling as a function of compressor speed when the EEV opening is adjusted to maximize the COP. As the compressor speed increases, the condensing pressure and refrigerant flow rate increase, while the evaporating pressure decreases. Besides, both subcooling and superheat increase with a rise of compressor speed due to an increase in the temperature difference between the refrigerant and secondary fluid in the evaporator and condenser. Therefore, the EEV opening has to be increased to obtain higher capacity and to reduce power consumption with a smaller compression ratio.

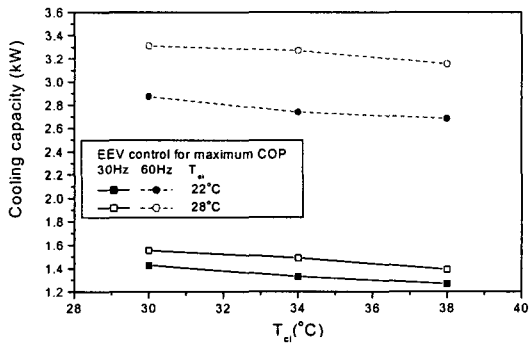

Fig. 4 Variation of capacity as a function of T_{ci}.

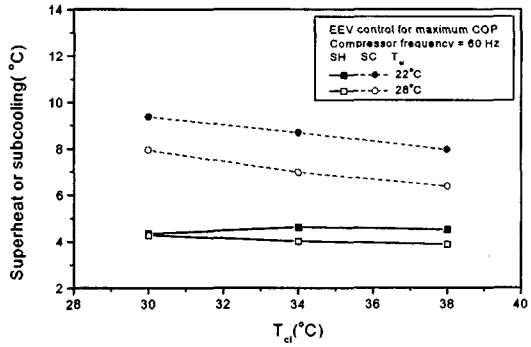

Fig. 5 Variation of superheat and subcooling as a function of T_{ci}.

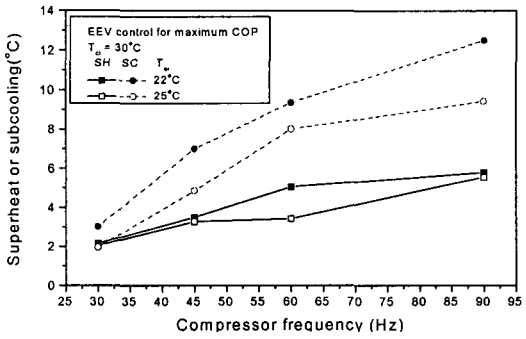

Fig. 6 Variation of superheat and subcooling as a function of compressor speed.

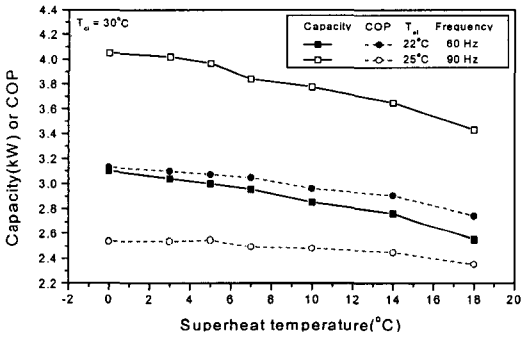

Fig. 7 Variation of capacity and COP as a function of superheat.

When the compressor speed varies, a superheat control may achieve better performance and higher stability as compared to subcooling control because the variation of superheat according to a compressor speed is much less than that of subcooling.

Fig. 7 represents the variations of cooling capacity and COP with respect to superheat that is resulted when the EEV opening is controlled. Cooling capacity and COP increase with a decrease of superheat due to a rise of heat exchanger efficiency. However, the slopes for cooling capacity and COP are gradually decreased as the superheat is reduced.

For the superheat above 5℃, the variation of COP with respect to superheat in the low frequency region is significantly greater than that in the high frequency region. The COP at a superheat of 18℃ is 11.7% and 7.7%, respectively, lower than those for an optimized cycle including optimal control of the EEV opening.

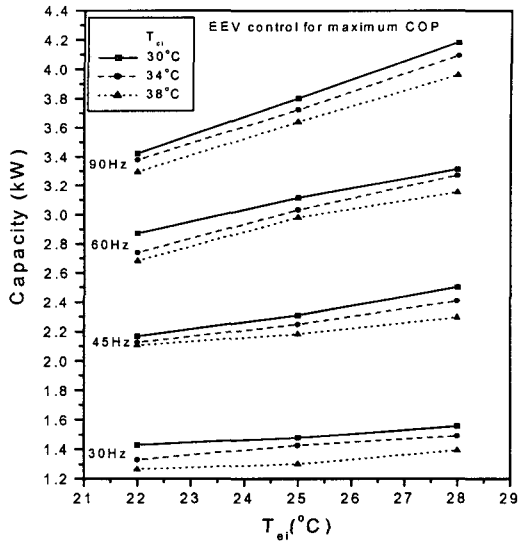

Fig. 8 Capacity chart of heat pump system.

As the frequency becomes higher, the increase of refrigerant mass flow rate become large as to EEV opening, which reduces degradation of COP due to a small variation of compression ratio at high frequencies. For superheat below 5℃, the variation of COP is less than 1.9%. Therefore, the EEV opening has to be optimally controlled to maintain the superheat below 5℃, which maximizes the COP and yields optimal system operation at all frequencies and load variations.

Fig. 8 represents the variation of capacity with respect to inlet temperature of secondary fluid in the evaporator and compressor speed when the EEV opening is adjusted to obtain a maximum COP. The most dominant factor affecting cooling capacity is compressor frequency among the operating parameters such as secondary fluid temperatures in the evaporator and condenser. The cooling capacity increases with a rise of compressor frequency, but the slope of capacity vs. frequency gradually decreases.

When the EEV opening was controlled to achieve a maximum COP at different operating

Table 2 Coefficient of Eq. (2)

Coefficients	Value	Coefficients	Value
a	39.77641	f	−2.05653
b	−0.76577	g	0.32334
c	−2.30016	h	0.01059
d	28.77707	i	0.11713
e	−0.01136	j	7.23153

conditions, cooling capacity was affected by compressor speed, and secondary fluid temperatures in the evaporator. Based on the experimental data, a correlation between compressor speed and cooling load was developed as given in Eq. (2). The predicted frequencies showed a good agreement with the test data with a maximum deviation of ±3%.

$$F = a + b \cdot T_{ci} + c \cdot T_{ei} + d \cdot \dot{Q}_{req} + e \cdot T_{ci} \cdot T_{ei} + f \cdot T_{ei} \cdot \dot{Q}_{req} + g \cdot \dot{Q}_{req} \cdot T_{ci} + h \cdot T_{ci}^2 + i \cdot T_{ei}^2 + j \cdot \dot{Q}_{req}^2 \quad (2)$$

In this study, the compressor speed was determined by indoor and outdoor loads. The cooling capacity was evaluated by using flow rate, inlet and outlet temperatures of secondary fluid in the evaporator. The coefficients given in Table 2 was determined by using a non-linear regression scheme.

4.2 Controller performance

Fig. 9 shows the response of superheat at different control gains when the system starts at 60 Hz with the PI feedback control algorithm. The system responds very quickly at a high proportional gain, but it requires more stabilization time.[10] When the integral gain is relatively high, an overshoot becomes large because the EEV opening varies very rapidly with a fast compensation of an error.[2] When the sampling time is decreased from 15 to 10 seconds, the control performance of the system is enhanced. However, as the sampling time is decreased from 10 to 5 seconds, the system performance is reduced due to over loads into the EEV. This would indicate that the control

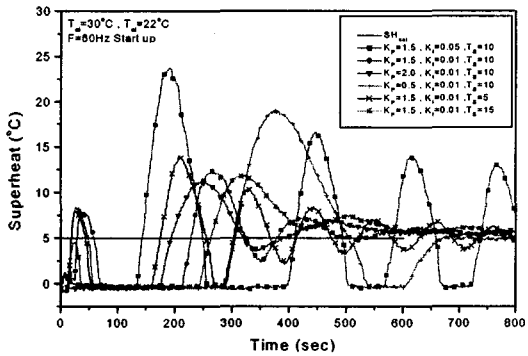

Fig. 9 Variation of superheat with respect to control gain at 60 Hz start up.

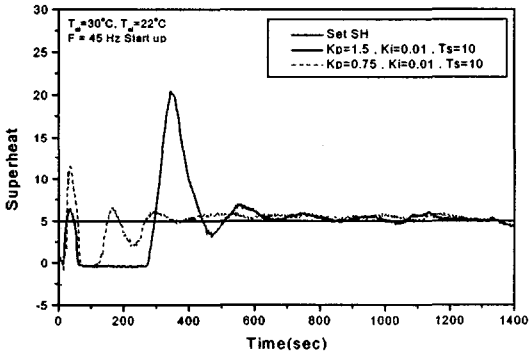

Fig. 10 Superheat as a function of time at 45 Hz start up.

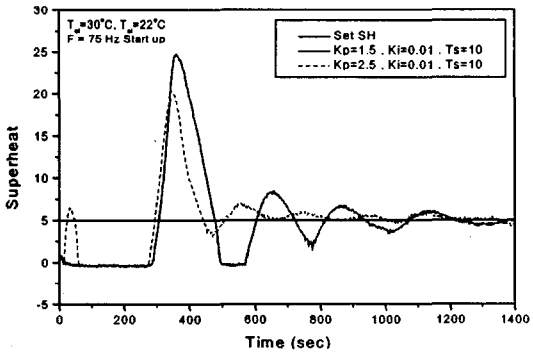

Fig. 11 Superheat as a function of time at 75 Hz start up.

performance of the system drops when the EEV operates at an excessively high speed. In this study, the time constant and time delay were selected at 27 and 10 seconds, respectively, from the test results of step changes in the system. Using the Ziegler-Nichols[2,13] tuning method, the proportional gain and integral gain were determined as 1.5 and 0.01, respectively.

Figs. 10 and 11 show the response of superheat when the system starts at 45 and 75 Hz with the optimum gain obtained at 60 Hz starting condition. The system at 45 Hz shows relatively small overshoot, and then quickly reaches stable operating conditions at a low proportional gain due to a small variation of flow rate. It is noticeable that the deviation during steady state operation with a variation of starting compressor frequency is not dependent on the control gain. Therefore, the system can be controlled appropriately at various compressor speeds using the same control gain determined at the rated frequency.

Fig. 12 shows the variation of secondary fluid exit temperature of the evaporator and EEV opening when the secondary fluid setting temperature of the evaporator exit is varied from 22℃ to 19℃. Compressor speed is adjusted with respect to the secondary fluid setting temperature of the evaporator using the correlation given in Eq. (2). The EEV opening is controlled to match the setting superheat by the PI feedback control algorithm. The relation between EEV opening and superheat showed nonlinear characteristics, which were also observed by Jung et al.[2] The evaporating temperature decreases with an increase of cooling load. However, the mean temperature difference between the refrigerant and secondary fluid in the evaporator increases due to a rise of compressor speed. The superheat increases significantly due to the delay of an increase in refrigerant flow rate. Therefore, in this case, more stabilization time is required, and wet

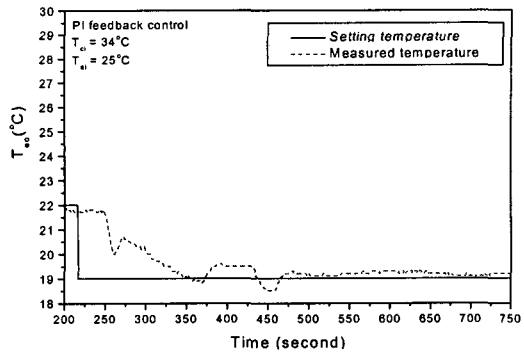

(a) Variation of T_{eo}

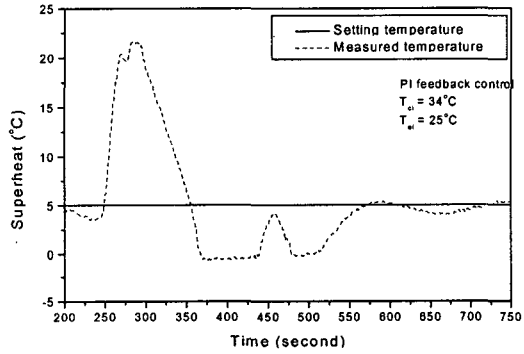

(b) Variation of superheat

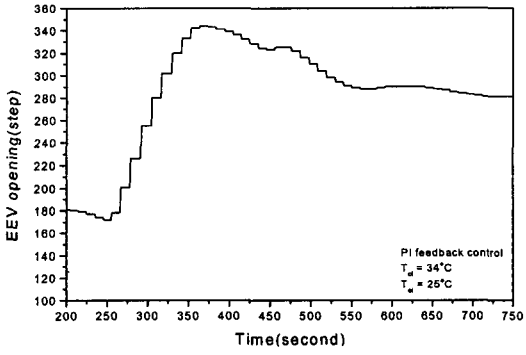

(c) Variation of EEV opening

Fig. 12 Results of PI feedback control.

compression can occur due to a higher output signal for the EEV opening to reduce the superheat. Therefore, when the cooling load is rapidly varied, a gradual controlling of compressor speed would be better to achieve higher system performance and reliability. However, it should be noted that an approaching

time to a setpoint is still relatively high because the variation of required cooling capacity is relatively small.

Fig. 13 represents the control performance of the system using the PI feedforward control algorithm. The EEV opening that corresponds to the change of compressor frequency is feedforwarded by using a correlation derived from the test results. When the compressor speed increases with a variation of operating conditions, the fluctuation of superheat is significantly reduced as compared to that observed in the simple PI feedback control (Fig. 12). In addition, the PI feedforward algorithm prevents wet compression by compensating the time delay in response to compressor frequency.

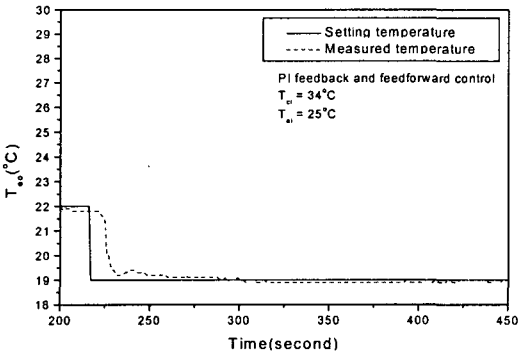

(a) Variation of T_{eo}

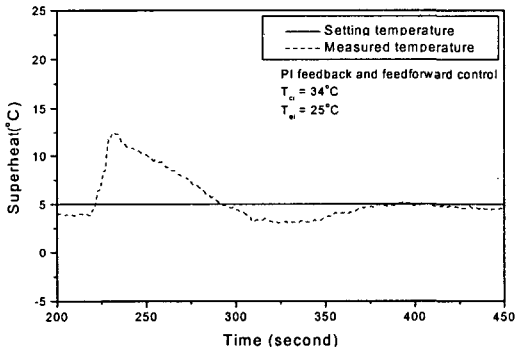

(b) Variation of superheat

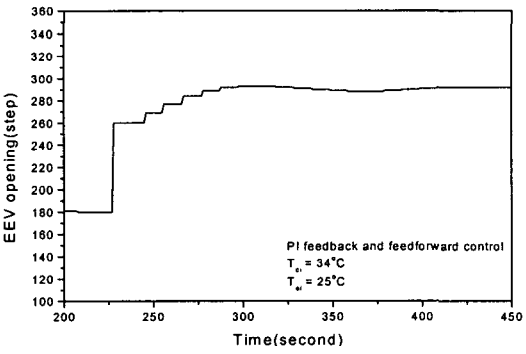

(c) Variation of EEV opening

Fig. 13 Results of PI feedback with feedforward control.

5. Conclusions

Performance tests of the inverter-driven water-to-water heat pump with EEV was executed. The controller using the PI feedback or PI feedforward algorithm was designed and tested. The test results can be summarized as follows.

(1) Controlling the superheat at the inlet of the compressor yielded higher efficiency and reliability of the system by adjusting compressor speed and EEV opening with a variation of the load.

(2) Although the relation between superheat and EEV opening of the heat pump showed nonlinear characteristics, a gain value obtained at the rated frequency was applicable to various operating conditions without causing large deviations.

(3) When the PI feedback control algorithm was applied at various compressor frequencies, a large overshoot of superheat and wet compression were observed due to time delay effects of compressor frequency.

(4) Applying the PI feedforward control scheme yielded better system performance and more reliable operation when compared to the PI feedback algorithm.

Acknowledgements

This work was supported by a grant No. 2000-908-E00011 from Korea Research Foun-

dation and grant No. 99-E-ID03-P-01 from Energy and Resources of the Korea Energy Management Corporation Foundation.

References

1. Riegger, O. K., 1988, Variable Speed Compressor Performance, OT-88-06-1.
2. Jung, D. S., Kim, M., Kim, M. S. and Lee, W., 2000, Capacity Modulation of a Multi-Type Heat Pump System Using PID Control, Korean J. of Air. and Ref. Eng., Vol. 12, No. 5, pp. 466-475.
3. Park, J. H., Park, Y. M., Hwang, Y. J. and Cho, K. S., 2000, A Study for Algorithm Optimization of the Inverter Driven Heat Pump with Electronic Expansion Valve, Proceedings of the SAREK Annual Summer Conference, pp. 514-519.
4. Kimura, N., 1986, Electric Expansion Valves, Refrigeration, Vol. 61, No. 701, pp. 231-238.
5. Higuchi, K., 1986, Evaporator Control Systems, Refrigeration, Vol. 61, No. 701, pp. 223-230.
6. Hewitt, N. J., McMullan, J. T., Murphy, N. E. and Ng, C. T., 1995, Comparison of Expansion Valve Performance, Int. J. of Energy Research, Vol. 19, pp. 347-359.
7. Matsuoka, F. and Nagatomo, H., 1988, Dynamic Response and Electrical Control for the Air Conditioner, Trans. of the JAR, Vol. 5, No. 1, pp. 43-54.
8. Nancy, B. M. S., 1990, Modeling and Simulation of a Water-to-Water Heat Pump Incorporating Superheat Control, M. S. Thesis, Univ. of Waterloo, Ontario, Canada.
9. McLinden, M. O., Klein, M. O., Lemmon, E. W. and Peskin, A. P., 1998, Thermo-dynamic and Transport Properties of Refrigerants and Refrigerant Mixtures (REFPROP 6.0), NIST, Gaithersburg, MD., U.S.A.
10. Ogata, K., 1970, Modern Control Engineering, 2nd ed., Prentice-Hall.
11. Yasuda, H., Ishibane, K. and Nakayama, S., 1992, Evaporator Superheat Control by an Electrically Driven Expansion Valve, Trans. of the JAR, Vol. 5, No. 2, pp. 147-156.
12. Franklin, G. F., Powell, J. D. and Workman, M. L., 1998, Digital Control of Dynamic Systems, 3rd ed., Addison Wesley.
13. Astrom, K. J. and Wittenmark, B., 1997, Computer-controlled Systems, 3rd ed., Prentice-Hall.